Supporting Information

A $NiCo_2O_4$ electrocatalyst with a thin graphitic coating for anion exchange membrane water electrolysis of wastewater

Jae-Yeop Jeong,[†a] Yoo Sei Park,[†b] Jaehoon Jeong,[a] Kyung-Bok Lee,[a] Dohyung Kim,[a] Ki-Yong Yoon,[a] Han-Seam Park,[c] Juchan Yang[*a]

[a] Department of Hydrogen Energy Materials, Surface & Nano Materials Division, Korea Institute of Materials Science (KIMS), Changwon, 51508, Republic of Korea

[b] Department of Advanced Material Engineering, Chungbuk National University, Chungdae-ro 1, Seowon-Gu, Cheongju, Chungbuk, 28644 Republic of Korea

[c] Mobility & IT Battery Division, LG Energy Solution, Daejeon, 34112, Republic of Korea

[†]These authors have contributed equally.

[*]Corresponding author

E-mail: jcyang@kims.re.kr (Dr. J.Y)

Keywords: electrocatalyst, carbon coating, waste water, hydrogen production, anion exchange membrane water electrolysis

Fig. S1. The photograph of weighing results of obtained electrocatalyst in the synthesis process.

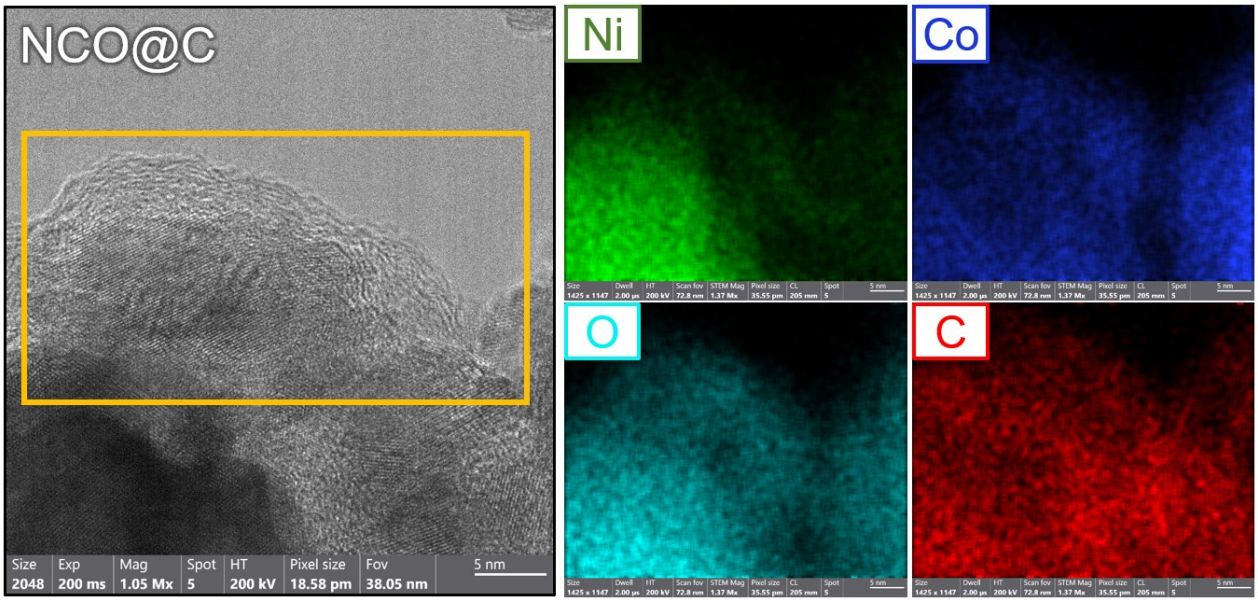

Fig. S2. Energy-dispersive spectroscopic mapping of NCO@C for elemental Ni, Co, O and C.

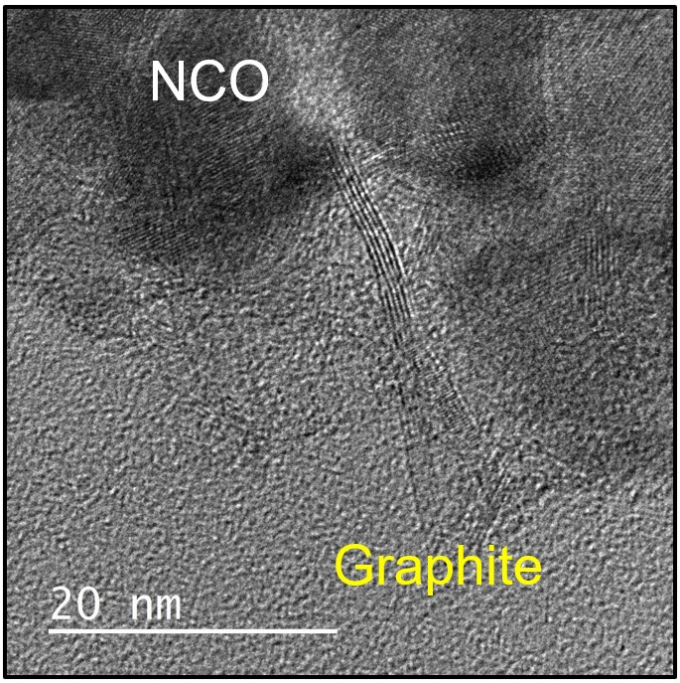

Fig. S3. TEM image of physically mixed NCO and graphite without ball-milling process.

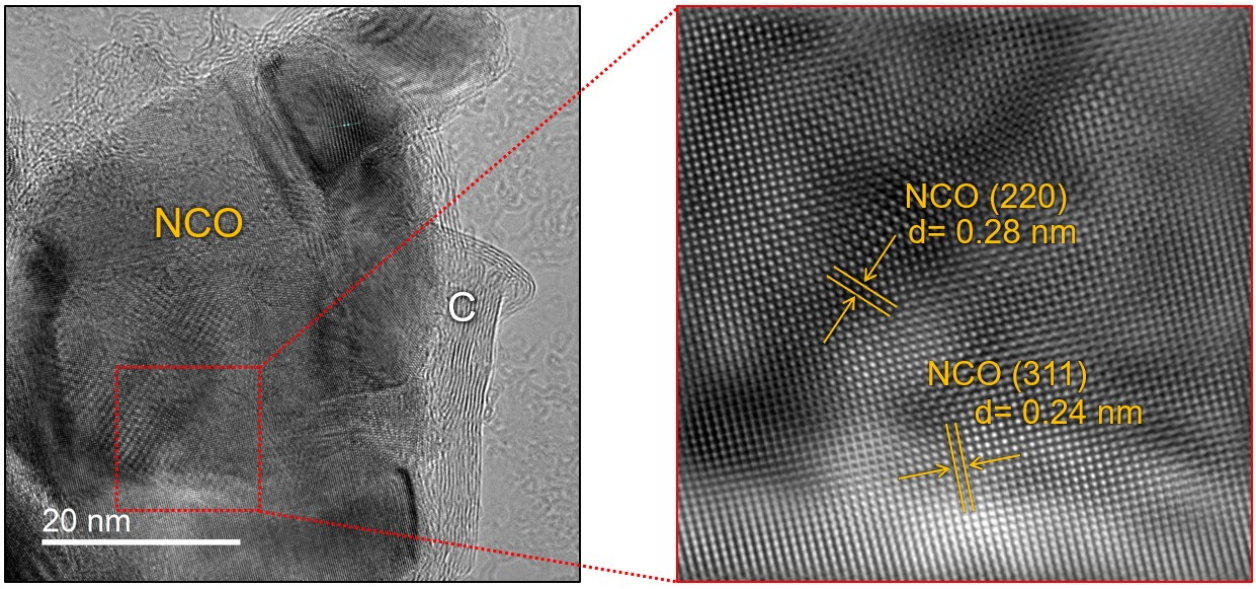

Fig. S4. TEM image of NCO@C. High resolution TEM image (right) taken from red part in NCO@C low magnification image (left). (NCO: $NiCo_2O_4$)

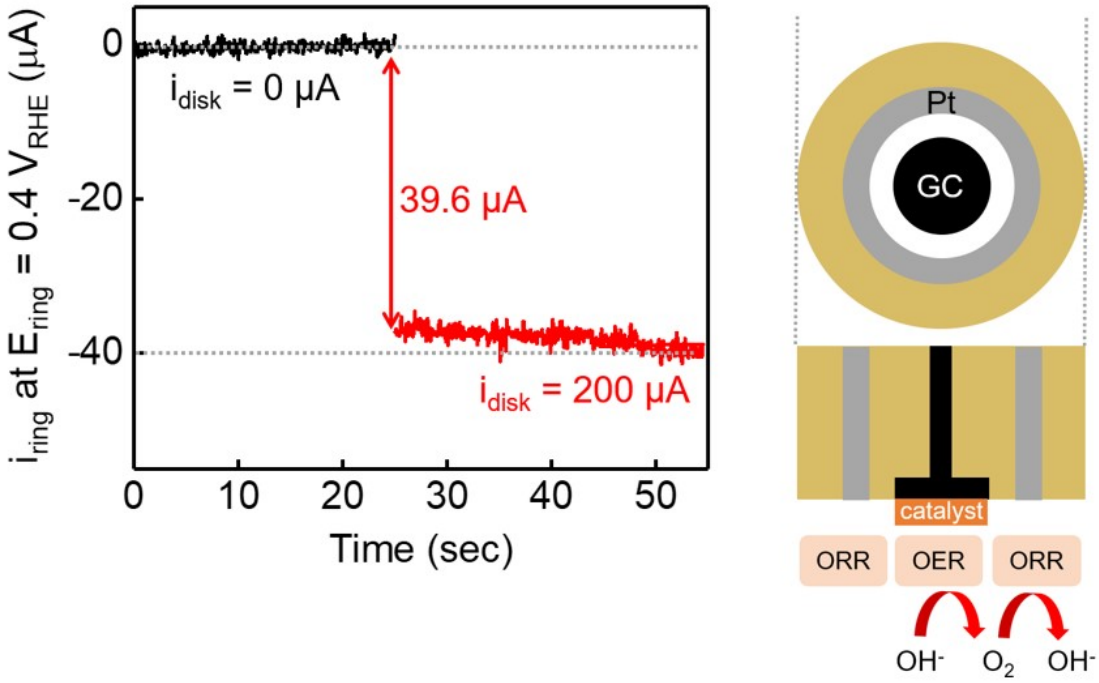

Fig. S5. RRDE testing of NCO@C for OER Faradaic efficiency (FE) in 0.1 M KOH solution. The schematic illustration (right) of using RRDE to measure the FE. OER process in GC disk electrode generates oxygen ($4OH^- \rightarrow O_2 + 4e^- + 2H_2O$), which is reduced by oxygen reduction reaction (ORR) at Pt ring electrode. The ring potential of 0.4 V_{RHE} was applied to reduce the generated oxygen, and OER in the disk electrode and ORR in the ring electrode occur successively. The FE was calculated as follow equation.

$$FE = I_{ring} / (I_{disk} \cdot N)$$

Where I_{disk} and I_{ring} are the disk and ring current, respectively. N represents the current collection efficiency of the Pt ring with the value of 0.2.

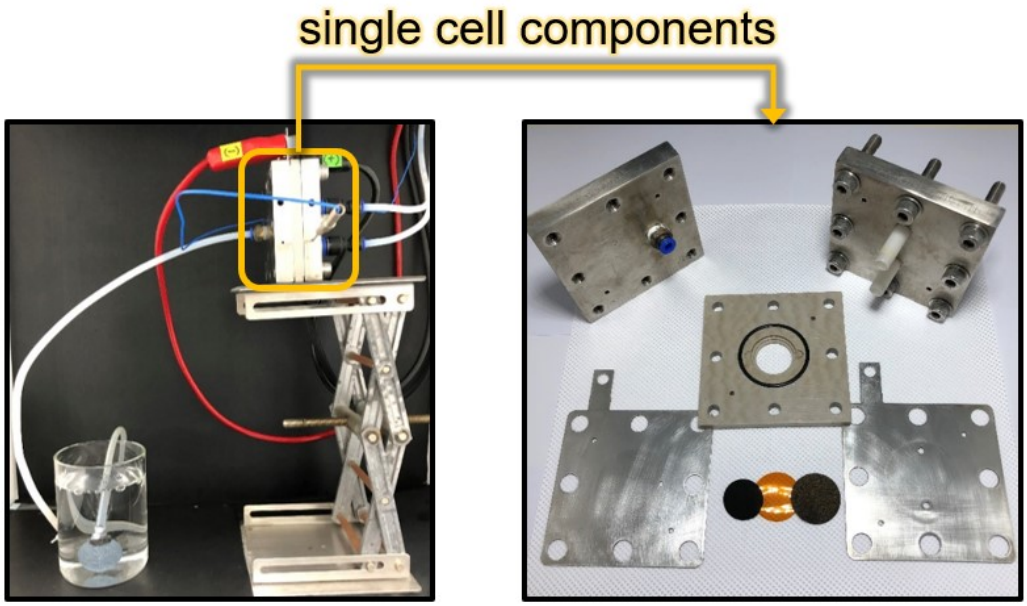

Fig. S6. The photograph of the AEMWE single cell operation (left) and unit configuration (right). The configuration of single cell is as follows: cathode ‖ AEM ‖ anode.

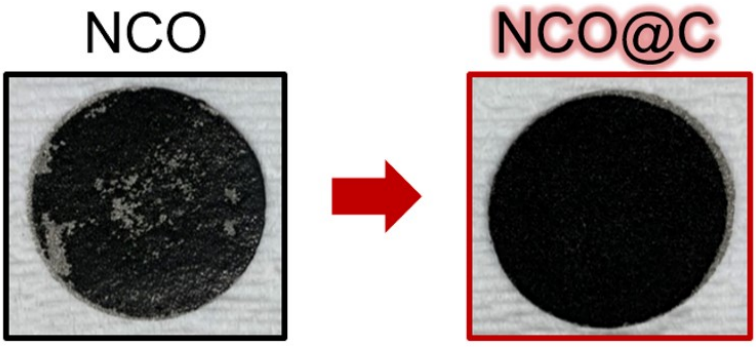

Fig. S7. Comparison of the surface of electrode with the same amount of synthetic electrocatalyst. On the electrode surface to which the NCO@C catalyst is applied, the carbon coating effect shows a uniform electrode surface.

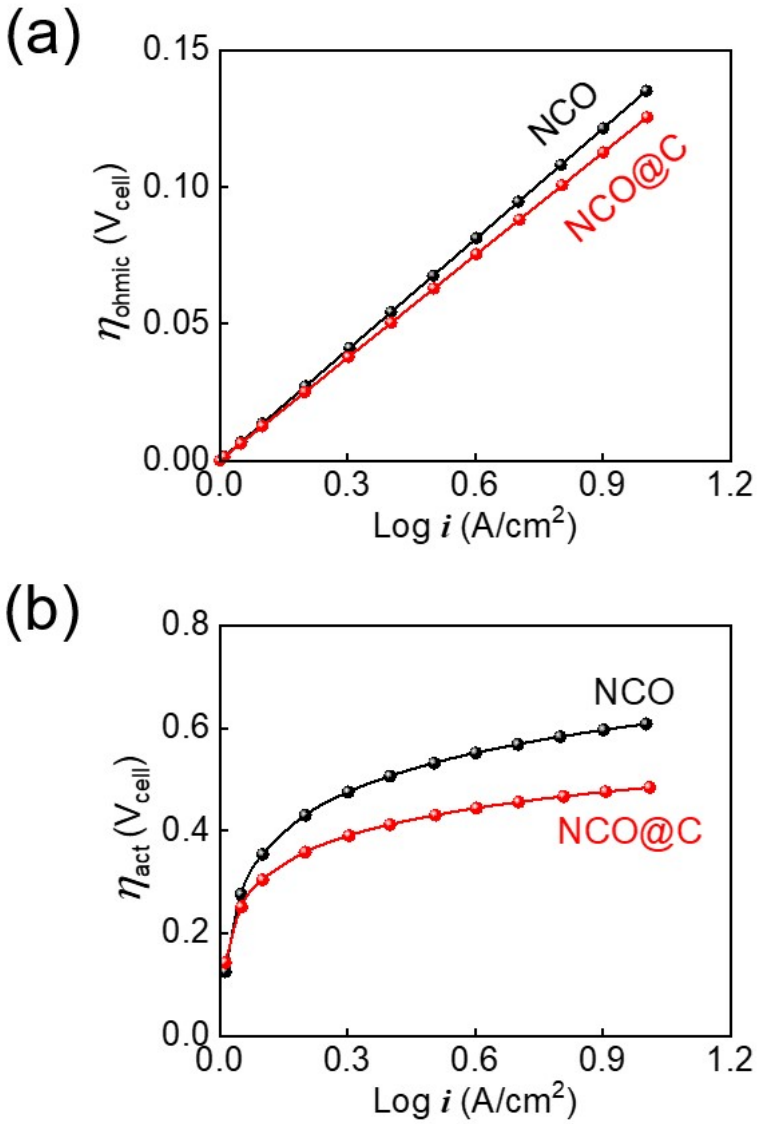

Fig. S8. The overpotential of AEMWE with NCO@C and NCO as anode was subdivide into (a) ohmic overpotential (η_{ohmic}) and (b) activation overpotential (η_{act}) at various current density region.

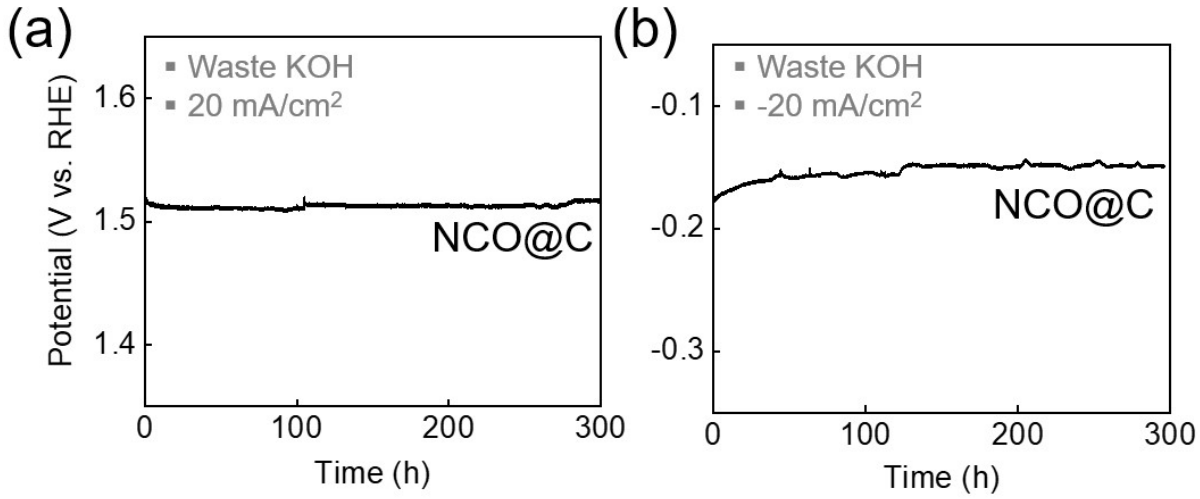

Fig. S9. Continuous long-term durability test of NCO@C electrocatalyst at 20 mA/cm^2 for OER (a) and -20 mA/cm^2 for HER (b) in waste KOH electrolyte.

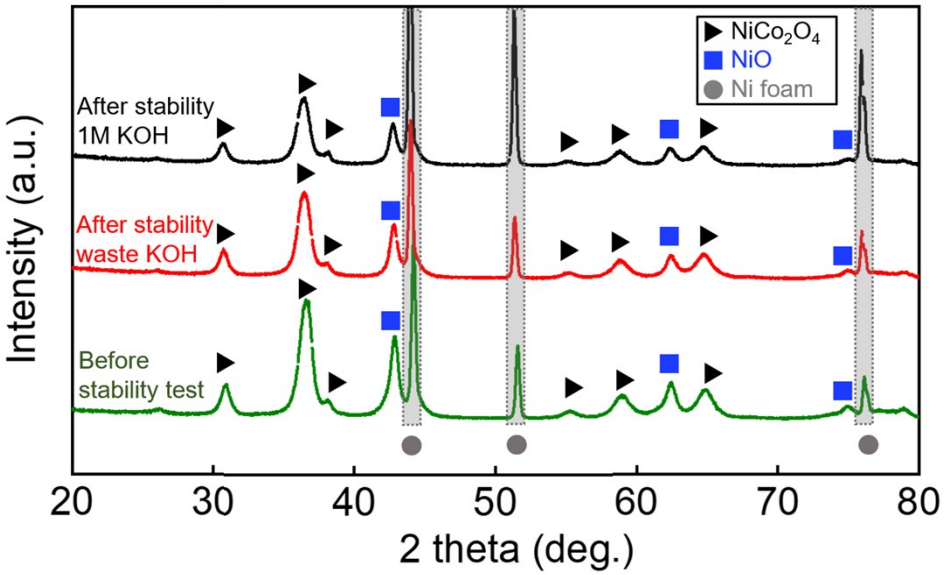

Fig. S10. XRD patterns of anode electrode applied NCO@C before and after durability test.

Table S1. Comparison of the performance of AEMWE single cell by non-precious electrocatalyst as anode and cathode.

Cathode	Anode	Electrolyte	Temperature (°C)	Performance	Reference
$NiCo_2O_4$	$NiCo_2O_4$	1M KOH	50	0.764 A/cm^2 at 1.9 V_{cell}	This work
$NiCo_2O_4$	$NiCo_2O_4$	Waste KOH	50	0.923 A/cm^2 at 1.9 V_{cell}	This work
NiFeCoP	NiFeCo-LDH	1M KOH	50	0.5 A/cm^2 at 1.75 V_{cell}	1
NiCo/NiCoO	$CuCo_2O_4$	1M KOH	50	0.5 A/cm^2 at 1.85 V_{cell}	2
Co_3S_4	$Cu_{0.81}Co_{2.19}O_4$	1M KOH	60	0.431 A/cm^2 at 2 V_{cell}	3
CoP	CoP	DI water	50	0.335 A/cm^2 at 1.8 V_{cell}	4
Ni/CeO_2-La_2O_3/C	$CuCoO_x$	0.1M NaOH	70	0.208 A/cm^2 at 2.2 V_{cell}	5
Ni	$Ce_{0.2}MnFe_{1.8}O_4$	1M KOH	25	0.3 A/cm^2 at 1.8 V_{cell}	6
Ni/CeO_2-La_2O_3/C	$CuCoO_x$	1M KOH	43	0.47 A/cm^2 at 1.9 V_{cell}	7
Ni	Ni	1M KOH	50	0.15 A/cm^2 at 1.9 V_{cell}	8
Ni	$Li_{0.21}Co_{2.79}O_4$	DI water	45	0.3 A/cm^2 at 2.05 V_{cell}	9
Ni	$Cu_{0.7}Co_{2.3}O_4$	1M KOH	55	0.1 A/cm^2 at 1.99 V_{cell}	10
NiMo	NiFe	DI water	70	0.4 A/cm^2 at 1.85 V_{cell}	11
Ni	$Cu_{0.7}Co_{2.3}O_4$	DI water	22	0.1 A/cm^2 at 1.9 V_{cell}	12

Reference for table S1.

1. J. Lee, H. Jung, Y. S. Park, N. Kwon, S. Woo, N. C. S. Selvam, G. S. Han, H. S. Jung, P. J. Yoo, S. M. Choi, J. W. Han and B. Lim, Applied Catalysis B: Environmental, 2021, 294, 120246.

2. Y. S. Park, J. Jeong, Y. Noh, M. J. Jang, J. Lee, K. H. Lee, D. C. Lim, M. H. Seo, W. B. Kim, J. Yang and S. M. Choi, Applied Catalysis B: Environmental, 2021, 292, 120170.

3. Y. S. Park, J. H. Lee, M. J. Jang, J. Jeong, S. M. Park, W.-S. Choi, Y. Kim, J. Yang and S. M. Choi, International Journal of Hydrogen Energy, 2020, 45, 36-45.

4. J. Chang, L. Liang, C. Li, M. Wang, J. Ge, C. Liu and W. Xing, Green Chemistry, 2016, 18, 2287-2295.

5. L. Zeng and T. S. Zhao, Nano Energy, 2015, 11, 110-118.

6. T. Pandiarajan, L. John Berchmans and S. Ravichandran, RSC Advances, 2015, 5, 34100-34108.

7. C. C. Pavel, F. Cecconi, C. Emiliani, S. Santiccioli, A. Scaffidi, S. Catanorchi and M. Comotti, Angewandte Chemie International Edition, 2014, 53, 1378-1381.

8. S. H. Ahn, B.-S. Lee, I. Choi, S. J. Yoo, H.-J. Kim, E. Cho, D. Henkensmeier, S. W. Nam, S.-K. Kim and J. H. Jang, Applied Catalysis B: Environmental, 2014, 154-155, 197-205.

9. X. Wu and K. Scott, International Journal of Hydrogen Energy, 2013, 38, 3123-3129.

10. Y.-C. Cao, X. Wu and K. Scott, International Journal of Hydrogen Energy, 2012, 37, 9524-9528.

11. L. Xiao, S. Zhang, J. Pan, C. Yang, M. He, L. Zhuang and J. Lu, Energy & Environmental Science, 2012, 5, 7869-7871.

12. X. Wu and K. Scott, Journal of Power Sources, 2012, 214, 124-129.